Applied Mathematics & Information Sciences
An International Journal

http://dx.doi.org/10.12785/amis/080644

The Implementation of LSMR in Image Deblurring

Hao Xu[1,2], *Ting-Zhu Huang*[1,*], *Xiao-Guang Lv*[3] *and Jun Liu*[1]

[1] School of Mathematical Sciences, University of Electronic Science and Technology of China, Chengdu, Sichuan, 611731, P. R. China
[2] Sichuan Jiuzhou Electric Group Co., Ltd, Mianyang, Sichuan, 621000, P. R. China
[3] School of Science, Huaihai Institute of Technology, Lianyungang, Jiangsu, 222005, P. R. China

Received: 14 Nov. 2013, Revised: 12 Feb. 2014, Accepted: 13 Feb. 2014
Published online: 1 Nov. 2014

Abstract: Image deblurring is a classic problem which has been extensively studied in image processing. The challenge of image deblurring is how to devise efficient and reliable algorithms for recovering the original, sharp image from a blurred and noisy one. In this paper, we consider the implementation of the LSMR method for computing an approximate solution of an ill-posed problem arising from image deblurring. When equipped with a stopping rule based on the discrepancy principle, the LSMR method acts as a regularization method. The numerical examples illustrate that the LSMR method is able to give restored images of higher quality with less computational effort than other widely used regularization methods.

Keywords: Image deblurring; LSMR; Regularization; Golub-Kahan iterative bidiagonalization

1 Introduction

In the process of recording image, there is more or less blurry that prevents us from producing an ideal sharp image [7,8,10,16,17,18]. For example, the blurring in image can arise from relative motion between the camera and the original scene, or an optical system that is out of focus in the recording of a digital image. Yet another type of blurring is due to variations caused by turbulence in the air. Besides, such blurring is not confined to optical images, for instance electron micrographs are corrupted by spherical aberrations of the electron lenses, and CT scans suffer from X-ray scatter. In these and similar situations, the inevitable result is that we record a blurred image. With the exception of these blurring effects, the noise influence always corrupts any recorded image.

In these situations we need to take such imperfections into account so that we are able to estimate an uncorrupted image from distorted and noisy one by using a mathematical model of the blurring process. The task of image deblurring is to reconstruct an approximation of the original image, given a blurred and noisy image and a point spread function (PSF). Mathematically, image deblurring can be modeled as a Fredholm integral equation of the first kind

$$g(x,y) = \int_a^b \int_a^b k(x,s;y,t) f(s,t) ds dt + e(x,y), \qquad (1)$$

where the function $g(x,y)$ is the observed image, $e(x,y)$ represents the additive noise, $f(s,t)$ is the original image, and $k(x,s;y,t)$ is the point spread function (PSF). The discretization of (1) leads to the following matrix-vector equation

$$\tilde{g} = Af + e, \qquad (2)$$

where A is an $n^2 \times n^2$ matrix representing the blurring phenomena, which can be constructed from the PSF and the imposed boundary condition, f is an n^2-dimensional vector representing the original image and $\tilde{g}$ is an n^2-dimensional vector representing the blurry and noisy image.

In the applications of image deblurring, since the noise-free image g is not available, instead, the vector $\tilde{g} = g + e$ is known, we expect to determine a solution of a noise-free problem

$$g = Af \qquad (3)$$

by solving an ill-posed problem

$$\tilde{g} = A\tilde{f}. \qquad (4)$$

In this work, $\delta = \|e\|$ representing the Euclid norm of the noise is assumed explicitly known. Since A is strictly ill-conditioned and has many singular values decay to zero, the exact solution of (4), if it exists, typically is not a meaningful solution f^* of (3) owing to the small noise e.

* Corresponding author e-mail: tingzhuhuang@126.com

In general, many regularization methods are considered to compute a slightly stabilized solution which is less sensitive to errors. Some popular direct methods such as TSVD, Wiener filtering and Tikhonov regularization can get an approximate solution of f^*. However, it is generally infeasible to calculate the QR factorization or the singular value decomposition (SVD) of A explicitly when A is very large. In this way, direct methods become impractical. Fortunately, iterative methods may be an alternative method for large scale ill-posed problems. As is well known, iterative methods such as CGLS, GMRES and LSQR equipped with a suitable stopping rule, are some of the most popular and powerful iterative regularization methods [1,3,11,12,13, 19,20,21]. For these iterative methods, the iterations can be identified as a regularization parameter. For a regularization parameter k, in the first k iterations, the methods converge to the solution f^*, and then suddenly start to diverge and the noise begins to dominate the solution. Hence, at this stage the iterations should be stopped to avoid interference from the noise components. There are different methods for finding this regularization parameter, such as the discrepancy principle, the L-curve and generalized cross validation. There is merit and demerit to each of these approaches. For instance, discrepancy principle requires the information of the noise level. Regarding generalized cross validation, the computation of the singular value decomposition for large scale problems is infeasible. For the L-curve, it has been advocated for many applications where no prior information about the noise is available. But it may be necessary to solve the corresponding linear systems for several regularization parameters.

It is shown that the LSQR method for image deblurring proceeds in two steps [3,14]. Firstly, the image deblurring problem is projected on an economical subspace which is computationally much more. Secondly, the standard techniques of regularization can be applied to the simplified problem. The LSMR method [4] being based on the Golub-Kahan iterative bidiagonalization is alike to the famous LSQR method. As reported in [4], the LSMR method is safer than LSQR method for solving linear systems and least-squares problems, since it is the analytical equal of the MINERES method which puts into use the corresponding normal equation, so that not only the $\|r_m\|$ is monotonically decreasing in practice, but also the quantities $\|Ar_m\|$ are monotonically decreasing where $r_m = \tilde{g} - A\tilde{f}_m$ is the residual for the current iterate $\tilde{f}_m$.

However, little is known about the performance of the LSMR method when it is applied to an ill-posed problem from image deblurring. In view of the advantage and characteristic of the LSMR comparing with the LSQR, in this research we consider the implementation of the LSMR iterative method combined with regularization for image deblurring problem with a stoping rule based on the discrepancy principle.

We summarize briefly the content of our paper. In Section 2, we give a brief recollection of the Golub-Kahan iterative bidiagonalization. In Section 3, we introduce the LSMR algorithm and discuss its application to an ill-posed problem from image deblurring. Numerical examples are provided in Section 4 to illustrate the satisfactory performance of the LSMR method. Conclusions are the subject of Section 5.

2 Golub-Kahan iterative bidiagonalization

In the section, we are going to review the Golub-Kahan iterative bidiagonalization [2] and its some properties that will be used in the LSMR method for solving ill-posed problems. At first, some notations that will be used throughout the paper. Let C, D... and u, v, ... denote matrices and vectors respectively, and α, β... denote scalars, in addition, we refer to a and b contenting with $a^2 + b^2 = 1$ as the significant components of a plane rotation matrix. $\|C\|$ and$\|u\|$ are used to denote the Frobenius norm of a matrix C and 2-norm of a vector u respectively.

According to a matrix A and a starting vector $\tilde{g}$, the Golub-Kahan iterative bidiagonalization could generate a sequence of vectors v_i and u_i, as well as scalars α_i and β_i such that A is reducing to lower bidiagonal form. A brief computational process of the method is described as follows.

Algorithm 1. Golub-Kahan iterative bidiagonalization

Input: A and $\tilde{g}$.

Output: two orthonormal bases $v_1, v_2, \cdots, v_m$ and $u_1, u_2, \cdots, u_m$, scalars $\alpha_1, \cdots, \alpha_m$ and $\beta_1, \cdots, \beta_{m+1}$.

$\beta_1 = \|\tilde{g}\|$, $u_1 = \tilde{g}/\beta_1$, $v_1 = A^T u_1$, $\alpha_1 = \|v_1\|$ and $v_1 = v_1/\alpha_1$.

for $i = 1, 2, \cdots, m$ do

$u_{i+1} = Av_i - \alpha_i u_i$;

$\beta_{i+1} = \|u_{i+1}\|$; if $\beta_{i+1} = 0$ stop;

$u_{i+1} = u_{i+1}/\beta_{i+1}$;

$v_{i+1} = A^T u_{i+1} - \beta_{i+1} v_i$

$\alpha_{i+1} = \|v_{i+1}\|$; if $\alpha_{i+1} = 0$ stop;

$v_{i+1} = v_{i+1}/\alpha_{i+1}$;

end do

Note that in Algorithm 1, $\alpha_i \geq 0$ and $\beta_i \geq 0$, $i = 0, 1, 2, ...$ are normalization constants chosen so that $\|u_{i+1}\| = \|v_{i+1}\| = 1$. In particular, $\beta_1 = \|\tilde{g}\|$. With the definitions

$$U_m = (u_1, u_2, \cdots, u_m), \quad V_m = (v_1, v_2, \cdots, v_m),$$

and

$$B_k = \begin{pmatrix} \alpha_1 & & & \\ \beta_2 & \alpha_2 & & \\ & \beta_3 & \ddots & \\ & & \ddots & \alpha_m \\ & & & \beta_{m+1} \end{pmatrix},$$

the recurrence relations in Algorithm 1 may be rewritten as

$$U_{m+1}(\beta_1 e_1) = \tilde{g},$$

$$\begin{cases} AV_m = U_{m+1}B_m \\ A^T U_{m+1} = V_m B_m^T + \alpha_{m+1} v_{m+1} e_{m+1}^T \end{cases}.$$

By straightforward computations, it is easy to observe that

$$A^T A V_m = V_m B_m^T B_m + \alpha_{m+1}\beta_{m+1} v_{m+1} e_m^T.$$

In fact, this is the equal of the result produced by the symmetric Lanczos process with regard to matrix $A^T A$.

3 The LSMR method

We begin this section by reviewing properties of the LSMR method. For further details and extensions of the method, we refer to the work by Fong and Saunders [4]. Introduce the Krylov subspaces

$$\mathscr{K}_m(A,\tilde{g}) = \text{span}\{\tilde{g}, A\tilde{g}, \cdots, A^{m-1}\tilde{g}\}, \quad m = 1,2,3\cdots.$$

Denote an approximate solution $\tilde{f}_m \in \mathscr{K}_m(A^T A, A^T \tilde{g})$ determined by applying m steps of the LSMR method to the linear system of equation (4). Then $\tilde{f}_m$ satisfies

$$\|A^T r_m\| = \min_{\tilde{f}\in\mathscr{K}_m(A^T A, A^T\tilde{g})} \|A^T(\tilde{g} - A\tilde{f})\|,$$

where $r_m = \tilde{g} - A\tilde{f}_m$ is the residual. It is obvious that the LSMR method is analytically equivalent to the MINRES method applied to the normal equation $A^T A\tilde{f} = A^T\tilde{g}$. Hence the quantities $\|A^T r_m\|$ are monotonically decreasing. In practice, Fong and Saunders have showed that $\|r_m\|$ also decreases monotonically. It follows that the approximate solutions determined by the LSMR method satisfy $\|\tilde{g} - A\tilde{f}_m\| \le \|\tilde{g} - A\tilde{f}_{m-1}\|$, $m = 1,2,3,\cdots$. Here the initial guess $\tilde{f}_0 = 0$.

For an ill-posed problem arising from image deblurring, if the associated residual error r_m is of norm smaller than or equal to $\gamma\delta$, where δ is the norm of the noise in the right-hand side vector $\tilde{g}$ and $\gamma \ge 1$ is a specified constant [11,12,13,15,17], we terminate the iterations and determine an approximate solution $\tilde{f}_m$, such that

$$\|A\tilde{f}_m - \tilde{g}\| \le \gamma\delta, \quad \|A\tilde{f}_{m-1} - \tilde{g}\| > \gamma\delta.$$

The residual error $A\tilde{f}_m - \tilde{g}$ is sometimes referred to as the discrepancy and this stopping criterion as the discrepancy principle; see [5,6] for a discussion of its properties.

The Golub-Kahan iterative bidiagonalization forms the basis of the implementation of the LSMR method. We now seek an approximate solution $\tilde{f}_m = V_m y_m$ for some y_m. Let $\bar{\beta}_m = \alpha_m\beta_m$ for all m. The minimization of $\|A^T r_m\|$ leads to the subproblem

$$\min_{y_m} = \|A^T r_m\| = \min_{y_m} \|\bar{\beta}_1 e_1 - \begin{pmatrix} \bar{B}_m^T B_m \\ \bar{\beta}_{m+1} e_m^T \end{pmatrix} y_m\|.$$

How to solve this least squares subproblem efficiently is the core of the LSMR algorithm.

We are in the position to describe the LSMR algorithm based on the discrepancy principle for an ill-posed problem arising from image deblurring.

Algorithm 2. The LSMR method with the discrepancy principle for image deblurring

Input: A, $\tilde{g}$, γ and δ.

Output: a good approximate solution $\tilde{f}_m$.

Start: $\beta_1 = \|\tilde{g}\|$; $u_1 = \tilde{g}/\beta_1$; $v_1 = A^T u_1$; $\alpha_1 = \|v_1\|$; $v_1 = v_1/\alpha_1$; $\bar{\alpha}_1 = \alpha_1$;

$\bar{\zeta}_1 = \alpha_1\beta_1$; $\rho_0 = 1$; $\bar{\rho}_0 = 1$; $\bar{c}_0 = 1$; $\bar{s}_0 = 0$; $h_1 = v_1$; $\bar{h}_0 = 0$; $\tilde{f}_0 = 0$;

$m = 0$;

Iterate:

while $\|r_m\| > \gamma\delta$ do

$m = m + 1$;

compute the mth basis vectors v_m and u_m, and update the matrix B_m by

Algorithm 1;

form the first QR factorization

$\rho_m = (\bar{\alpha}_m^2 + \beta_m^2)^{\frac{1}{2}}$;

$c_m = \bar{\alpha}_m/\rho_m$; $s_m = \beta_{m+1}/\rho_m$;

$\theta_{m+1} = s_m\alpha_{m+1}$; $\bar{\alpha}_{m+1} = c_m\alpha_{m+1}$;

perform the second QR factorization

$\bar{\theta}_m = \bar{s}_{m-1}\rho_m$; $\bar{\rho}_m = ((\bar{c}_{m-1}\rho_m)^2 + \theta_{m+1}^2)^{\frac{1}{2}}$;

$\bar{c}_m = \bar{c}_{m-1}\rho_m/\bar{\rho}_m$; $\bar{s}_m = \theta_{m+1}/\bar{\rho}_m$;

$\zeta_m = \bar{c}_m\bar{\zeta}_m$; $\bar{\zeta}_{m+1} = -\bar{s}_m\bar{\zeta}_{m+1}$;

form the approximate solution

$\bar{h}_m = h_m - (\bar{\theta}_m\rho_m/\rho_{m-1}\bar{\rho}_{m-1})\bar{h}_{m-1}$;

$\tilde{f}_m = \tilde{f}_{m-1} + (\zeta_m/(\rho_m\bar{\rho}_m))\bar{h}_m$;

$r_m = \tilde{g} - A\tilde{f}_m$

$h_{m+1} = v_{m+1} - (\theta_{m+1}/\rho_m)h_m$;

end do

4 Numerical examples

This section presents several computed examples which illustrate the effectiveness of the LSMR method for the image deblurring problems. All computations were carried out in Matlab 7.0. In all tests, the black image (zero matrix) is the initial guess. The LSMR method is terminated as soon as an approximate solution that satisfies the discrepancy principle was computed. In the discrepancy principle, we choose $\gamma = 1.05$.

The aim of our first example is to give evidence of the usefulness of the LSMR method for computing the approximate solution of equation (4) from image deblurring. This numerical example is a test problem which is popular in the literature concerned with medical image processing [22,23]. The true image is 128×128 simulated MRI of a human brain, available in the the Matlab Image Processing Toolbox. To generate the distorted image, convolve the Guassian PSF making use of the function *psfGauss* in [24] with the MRI image, then add 2% Gaussian noise to the result with the built-in MATLAB function *randn*. The test data used in this

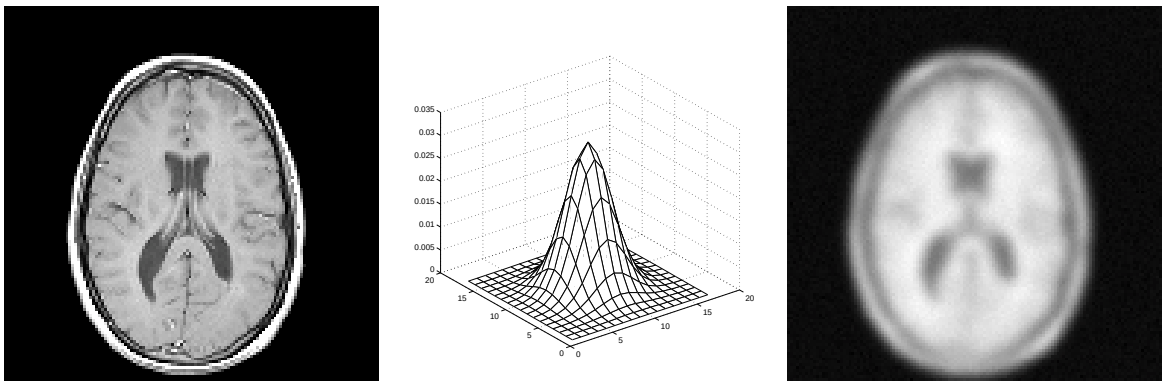

Fig. 1: True image (*left*), the Gaussian PSF (*center*) and the blurred and noisy image (*right*).

example is shown in Figure 1. The symmetric truncated Guassian PSF given by

$$h_{ij} = \begin{cases} ce^{-0.1(i^2+j^2)} & \text{if } |i-j| \le 8, \\ 0 & \text{otherwise,} \end{cases}$$

where c is the normalization constant.

For a bandlimited image deblurring, one must make full use of not only the image in the Field of View (FOV) of the given observation but also part of the scenery in the area bordering it [29]. Given the imposed boundary conditions, the blurring matrix A should reflect special structure. In practice, different boundary condition is selected for algebraic simpleness and computational convenience. For example, with the periodic boundary condition, the matrix A has a block circulant with circulant blocks (BCCB) structures, and the computation will be efficient by making use of the fast Fourier transforms (FFTs); the zero boundary condition produce a block Toeplitz with Toeplitz blocks (BTTB) blurring matrix. Although direct methods cannot be carried out efficiently, it is applicable to put iterative methods to use, since matrix-vector multiplications involving BTTB matrices can be implemented efficiently by FFTs; In the case of the reflexive boundary condition, the matrix A will transform into a block Toeplitz-plus-Hankel with Toeplitz-plus-Hankel blocks (BTHTHB) structure. For any symmetric PSF, the resulting matrix A can be diagonalized by the discrete cosine transform (DCT III) matrix; For the antireflexive boundary condition, the matrix A is a block Toeplitz plus Hankel plus 2 rank correction matrix. Owing to the design, the resulting matrices from symmetric PSFs can be diagonalized by the discrete sine transform (DST I) matrices; check [9,24,25, 26] for more details.

In this test, we consider solving image restoration by the LSMR method under four different boundary conditions. Since the original image f^* is available, we can evaluate the LSMR method by the relative error. Relative error of the restored image is denoted as $\|\tilde{f}_m - f^*\|_2/\|f^*\|_2$, where f^* denotes the original image and $\tilde{f}_m$ is the restored image obtained by regularization methods with truncation parameter m. Besides, another main term of comparison is the peak signal-to-noise ratio(PSNR) defined as $\mathrm{PSNR} = 10\log_{10}\frac{255^2 n^2}{\|\tilde{f}_m - f^*\|_F^2}$, where n is the size of the restored image .

In Table 1, we give the numbers of iterations for obtaining the restored images by the LSMR method with the four different BCs. Besides, the relative error and the PSNR for Test 1 are shown in Table 1. We denote the original PSNR and original relative error by ori_PSNR and ori_rel_err. From Table 1, we can see that the relative error computed by the LSMR method are much smaller than the relative error of the contaminated image. The LSMR method under the four BCs displays a higher PSNR than the blurred and noisy image. The computed images by the LSMR method are displayed in Figure 2. From Figure 2, we observe that the restored images that satisfy the discrepancy principle by the LSMR method with the four BCs are all better than the blurred and noisy image. The results of the four BCs state that the LSMR method can restore the images and suppress the noise magnification effectively.

In Test 2, we illustrate the efficiency of employing the LSMR method for image deblurring problems over the other two popular regularization methods (truncated singular value decomposition and Tikhonov regularization). The second test data we use is shown in Figure 3. In the true 168×168 image, the original 128×128 image f^* to be deblurred is delimited by white lines. In the test, the natural boundary condition will be considered contributing to the blur. We produce the blurring image by performing the blurring operation on a true image and adding 2% Gaussian white noise, from which a central part is cut out. Here the PSF we consider is the out-of-focus PSF constructed by using the function $psfDefocus$ in [24] with $r = 3$, $dim = 7$.

In this test, we consider two widely used BCs: reflexive BC and antireflexive BC. For the truncated singular value decomposition method (TSVD) and the

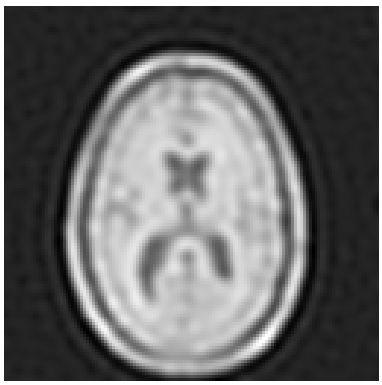

(a) LSMR method with the zero BC

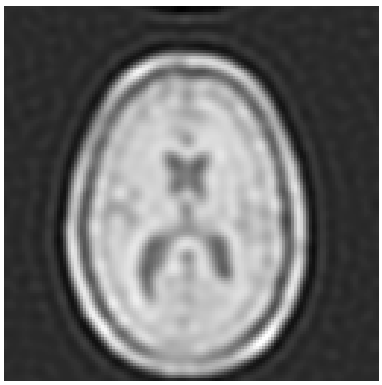

(b) LSMR method with the periodic BC

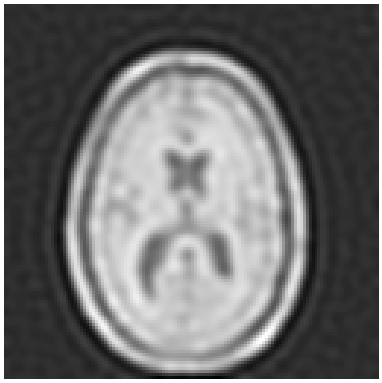

(c) LSMR method with the reflexive BC

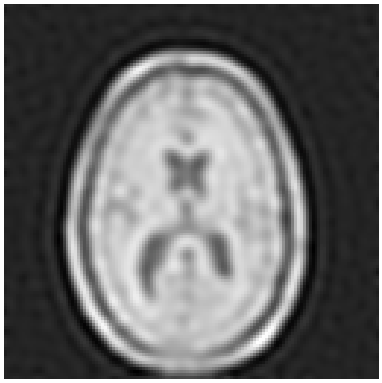

(d) LSMR method with the antireflexive BC

Fig. 2: Restored images obtained by the LSMR with four different boundary conditions

Table 1: Iterations, relative error, PSNR for the LSMR method with four different BCs.

	Zero BC	Periodic BC	Reflexive BC	Antireflexive BC
Iterations	13	14	13	13
Relative error	0.2376	0.2361	0.2377	0.2388
Ori_rel_err	0.3054			
PSNR	34.9355	34.9911	34.9328	34.8927
Ori_PSNR	32.7556			

Table 2: The relative error and PSNR by three different methods with different BCs.

BCs	Method	Relative error	PSNR
Reflexive	LSMR	0.1337	31.4151
	TSVD	0.1527	30.2618
	Tikhonov	0.1624	29.8384
Antireflexive	LSMR	0.1369	31.2109
	TSVD	0.1603	29.7301
	Tikhonov	0.1624	29.4934

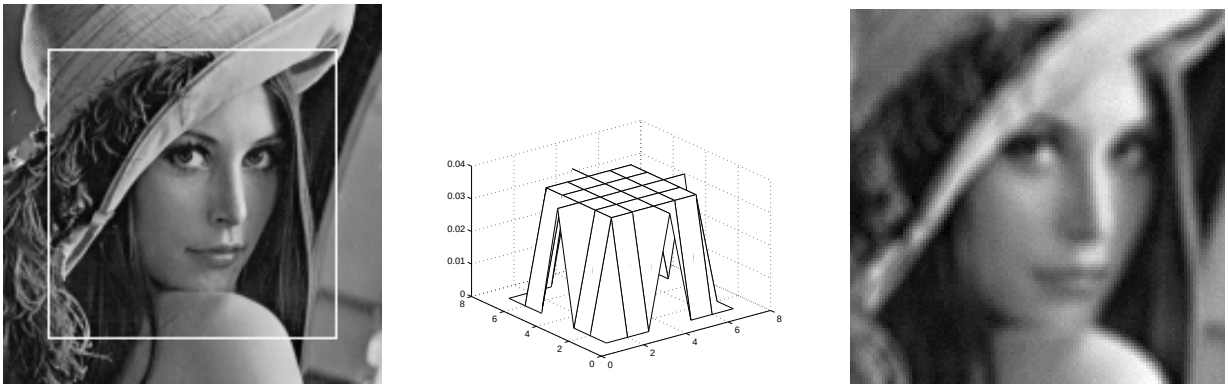

(a) True image (b) The out-of-focus PSF (c) Observed image

Fig. 3: True image, PSF and observed image of Test 2.

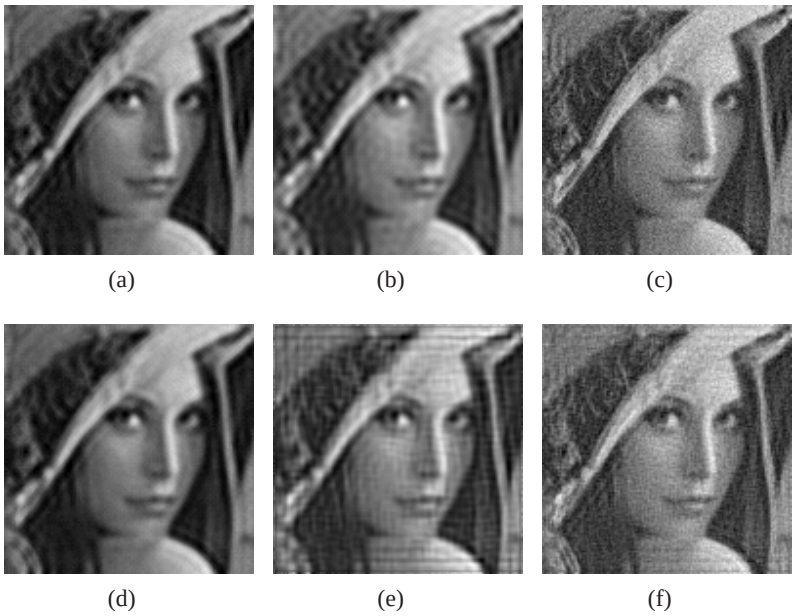

(a) (b) (c)

(d) (e) (f)

Fig. 4: Restored images for three different methods with two BCs of Test 2. (a) The approximate image determined after 8 steps of the LSMR method with the reflexive BC, (b) TSVD with the reflexive BC, (c) Tikhonov regularization method with the reflexive BC, (d) The approximate image determined after 7 steps of the LSMR method with the antireflexive BC, (e) TSVD method with the antireflexive BC, (f) Tikhonov regularization method with the antireflexive BC.

Tikhonov regularization method, we apply the generalized cross validation (GCV) to find their regularization parameters based on the Kronecker product approximation method; see [24,27,28].

The relative error and PSNR of the restored images by the three different methods are shown in Table 2. The relative error and PSNR of the observed image are ori_rel_err=0.1815 and ori_PSNR=28.7595. From Table 2, we see that under the two BCs, the relative error by the LSMR method with discrepancy principle is smaller than that by the TSVD method and the Tikhonov regularization method with GCV method obtaining regularization parameter, while the PSNR by the LSMR method is higher than that by the TSVD method and the Tikhonov regularization method. For the LSMR method, the stopping rule based on the discrepancy principle is satisfied after 8 steps under the reflexive BC and after 7 steps under the antireflexive BC. We remark that the computation of 8 steps under the reflexive BC and 7 steps under the antireflexive BC require the evaluation of 16 matrix-vector products and 14 matrix-vector products with the matrix A respectively, while the TSVD method

and the Tikhonov regularization method need the singular value decomposition of the matrix A of size $n^2 \times n^2$.

In Figure 4, we show the restored images using the LSMR method, the TSVD method and the Tikhonov regularization method under the two BCs for Test 2. It is easy to see from Figure 4 that the LSMR method can give restored images of higher quality than the other two popular methods. As expected, the LSMR method under the two BCs has addressed the problem of ringing effects at the image boundary.

5 Concluding remarks

This paper first discusses the properties and advantages of the LSMR iterative method. Two numerical examples are given to illustrate the performance of the scheme for computing the approximate solutions of large-scale ill-posed problems arising from image delurring. In order to be able to exhibit the effectiveness of the LSMR method, a comparison among the LSMR and the other two widely used methods is considered in the numerical test. Experiment results are provided to show the satisfactory performance of the LSMR method for image deblurring, with respect to the quality of the restored images and the computational saving.

Acknowledgement

The authors would like to express their great gratitude to Editor-in-Chief Prof. M. Abdel-Aty and the referees for their constructive comments and suggestions that lead to improvement of this paper. This research is supported by 973 Program (2013CB329404), NSFC (61370147), Chinese Universities Specialized Research Fund for the Doctoral Program (20110185110020), Sichuan Province Sci. & Tech. Research Project (2012GZX0080).

References

[1] C. C. Paige and M. A. Saunders, Algorithm 583; LSQR: Spares linear equations and least-squares problems, ACM Trans. Math. Softw., **8**, 195-290 (1982).
[2] G. H. Golub and W. Kahan, Calculating the singular values and pseudo-inverse of a matrix, J. of the Society for Industrial and Applied Mathematics, Series B: Numerical Analysis, **2**, 205-224 (1965).
[3] C. C. Paige and M. A. Saunders, LSQR: An algorithm for sparse linear equations and sparse least squares, ACM Trans. Math. Software, **8**, 43-71 (1982).
[4] D. C. Fong and M. A. Saunders, LSMR: An iterative algorithm for sparse least-squares peoblems, SIAM. J. Sci. Comput, **33**, 2950-2971 (2011).
[5] P. C. Hansen, Rank-Deficient and discrete ill-posed problems, SIAM, Philadelphia, (1998).
[6] V. A. Morozov, On the solution of functional equations by the methos of regularization, Soviet Math. Dokl., **7**, 414-417 (1966).
[7] A. Bovik, Handbook of image and video processing, Second Edition, Elsevier Academic Press, (2005).
[8] P. C. Hansen, J. G. Nagy and D. P. O'Leary, Deblurring Images: Matrices, Spectra, and Filtering, SIAM, Philadelphia, (2006).
[9] H. Andrew and B. Hunt, Digital Image Restoration, Prentice-Hall, Englewood Cliffs, NJ, (1977).
[10] M. R. Banham and A. K. Katsaggelos, Digital image restoration, IEEE Signal Processing Magazine, **14**, 24-41 (1997).
[11] M. Hanke, Conjugate Gradient Type Methods for Ill-Posed Problems, Longman, Harlow, (1995).
[12] D. Calvetti, B. Lewis, and L. Reichel, GMRES-type methods for inconsistent systems, Linear Algebra Appl., **316**, 157-169 (2000).
[13] D. Calvetti, B. Lewis, and L. Reichel, On the regularizing properties of the GMRES method, Numer. Math., **91**, 605-625 (2002).
[14] D. P. O'Leary and J. A. Simmons, A bidiagonalization-regularization porcedure for large scale discretizations of ill-posed problems, SIAM J. Sci. Statist. Comput., **2**, 474-489 (1981).
[15] D. Calvetti and G. Landi, L. Reichel and F. Sgallari, Non-negativity and iterative methods for ill-posed problems, Inverse Problems, **20**, 1747-1758 (2004).
[16] H. Engl, M. Hanke, and A. Neubauer, Regularization of Inverse Problems, Kluwer Academic Publishers: The Netherlands, (1996).
[17] P. C. Hansen, Rank Defficient and Discrete Ill-posed Problems: Numerical Aspects of Linear Inversion, SIAM: Philadelphia, PA, (1997).
[18] P. C. Hansen, Discrete Inverse Problems: Insight and Algorithms, SIAM, Philadelphia, (2010).
[19] M. Hanke, J. G. Nagy, and R. J. Plemmons. Preconditioned iterative regularization for ill-posed problems. In L. Reichel, A. Ruttan, and R. S. Varga, editors, Numerical Linear Algebra, de Gruyter, Berlin, 141-163 (1993).
[20] F. Benvenuto, R. Zanella, L. Zanni, and M. Bertero, Nonnegative least-squares image deblurring: improved gradient projection approaches, Inverse Problems, **26**, 025004 (2010).
[21] S. Bonettini, R. Zanella, and L. Zanni, A scaled gradient projection method for constrained image deblurring, Inverse Problems, **25**, 015002 (2009).
[22] V. N. Strakhov and S. V. Vorontsov, Digital image deblurring with SOR, Inverse Problems, **24**, 025024 (2008).
[23] J. G. Nagy, K. Palmer, and L. Perrone, Iterative methods for image deblurring: a Matlab object-oriented approach, Numer. Algorithms, **36**, 73-93 (2004). http://www.mathcs.emory.edu/nagy/RestoreTools.
[24] P. C. Hansen, J. G. Nagy, and D. P. OLeary, Deblurring Images: Matrices, Spectra, and Filtering, SIAM, Philadelphia, (2006).
[25] M. K. Ng., R. Chan, and W. C. Tang, A fast algorithm for deblurring models with Neumann boundary conditions, SIAM J. Sci. Comput., **21**, 851-866 (2000).
[26] S. S. Capizzano, A note on anti-reflective boundary conditions and fast deblurring models, SIAM J. Sci. Comput., **25**, 1307-1325 (2003).

[27] J. G. Nagy, M. K. Ng, and P. Lisa, Kronecker product approximations for image restoration with reflexive boundary conditions, SIAM J. Matrix Analysis Appl., **25**, 829-841 (2003).
[28] P. Lisa, Kronecker product approximations for image restoration with anti-reflective boundary conditions, Numer. Linear Algebra Appl., **13**, 1-22 2006.
[29] X.-G. Lv, T.-Z. Huang, Z.-B. Xu, X.-L. Zhao, A special Hermitian and skew-Hermitian splitting method for image restoration, Appl. Math. Modelling, **37**, 1069-1082 (2013).
[30] X.-G. Lv, T.-Z. Huang, Z.-B. Xu, X.-L. Zhao, Kronecker product approximations for image restoration with whole-sample symmetric boundary conditions, Information Sciences, **186**, 150-163 (2012).

Hao Xu received the M.Sc. degree in Computational Mathematics from University of Electronic Science and Technology of China, Chengdu, Sichuan, China, in 2009 and 2012. His research interests include numerical linear algebra with applications and variational methods in image processing.

Ting-Zhu Huang received the B. S., M. S., and Ph. D. degrees in Computational Mathematics from the Department of Mathematics, Xian Jiaotong University, Xian, China. He is currently a professor in the School of Mathematical Sciences, UESTC. He is currently an editor of The Scientific World Journal, Advances in Numerical Analysis, J. Pure and Appl. Math.: Adv. and Appl., J. Electronic Sci. and Tech. of China, etc. His current research interests include numerical linear algebra and scientific computation with applications, iterative methods of linear systems, numerical algorithms for image processing, preconditioning technologies, and matrix analysis with applications, etc.

Xiao-Guang Lv received the B.S. degree in mathematics at China University of Geosciences, Wuhan, Hubei, China, in 2002. He obtained his M.Sc. degree in mathematics and the Ph.D. degree in computational mathematics from University of Electronic Science and Technology of China, Chengdu, Sichuan, China, in 2007 and 2011, respectively. His research interests include numerical linear algebra with applications and variational methods in image processing.

Jun Liu received the B.S. degree in Information and Computing Sciences from Nanchang University, Nanchang, Jiangxi, China, in 2009. He is pursuing the Ph.D. degree at the University of Electronic Science and Technology of China, Chengdu, Sichuan, China. His research interests include the scientific computation and variational methods in image processing.